Oxanosine Is a Substrate of Adenosine Deaminase. Implications for the Quest for a Toxicological Marker for Nitrosation Activity

Papiya Majumdar,[§] Hong Wu,[§] Peter Tipton,*[,‡] and Rainer Glaser*[,§]

Departments of Chemistry and Biochemistry, University of Missouri−Columbia, Columbia, Missouri 65211

Received August 19, 2005

Oxanosine **3r**, 5-amino-3-*β*-(D-ribofuranosyl)-3*H*-imidazo[4,5-*d*][1,3]oxazine-7-one, was isolated as a novel nucleoside antibiotic in 1981 from *Streptomyces capreolus* MG265-CF3. Oxanosine became relevant in toxicology in 1996 with the discovery that it is formed in nitrosative guanosine deamination. As part of studies of the mechanism of oxanosine formation, the synthesis was attempted of [7-^{18}O]oxanosine by enzymatic ^{16}O/^{18}O-exchange with adenosine deaminase (ADA) in analogy to the synthesis of [6-^{18}O]guanosine from 2-amino-6-chloropurine. Unexpectedly, it was discovered that the incubation of oxanosine **3r** with ADA in sodium phosphate buffer (pH = 7.4) results in 1-*β*-(D-ribofuranosyl)-5-ureido-1*H*-imidazole-4-carboxylic acid **4r**. The reaction of the 2′-deoxyribose derivative **3d** forms **4d** in analogy. The reaction products were separated by preparative RP-HPLC and characterized by LC/MS and MS/MS analyses and UV/vis and NMR spectroscopy, and NMR assignments were corroborated by GIAO and GIAO−PCM calculations. Reaction in $H_2{}^{18}O$ leads to ^{18}O-incorporation at C7. The hydrolysis of **3** to **4** can be rationalized on the basis of the known mode of action of ADA, and an explanation is provided for ADA's accomplishment of the "usual" substitution at C6 of adenosine (addition to the exocyclic bond) and the "lactone hydrolysis" of oxanosine (addition to the endocyclic double bond). The Michaelis−Menten constant of K_m = 1.0 (±0.2) mM was measured for oxanosine. Implications are discussed for studies of nitrosative deamination of nucleosides, nucleotides, and oligonucleotides.

Introduction

The ingestion or inhalation of nitrosating reagents contained in foods (*1*, NO_x^-) or the environment (*2*, NO_x) have been known to cause in vivo nitrosation. The significance of this knowledge greatly increased with the discovery of endogenous NO synthesis (*3*), the recognition of the role of NO in the regulation of many biological processes (*4*), and the emergence of NO-releasing drugs (*5*) and NO-synthase inhibitors (*6*). And, most recently, increasing attention has focused on NO generated by deprotonation of HNO and subsequent oxidation of NO^- (*7*). Endogenous nitrosation involves N_2O_3, the anhydride of HNO_2 and the autoxidation product of NO (*8*), or peroxynitrite $ONOO^-$ (*9*), the superoxide adduct of NO, leads to DNA base deamination and interstrand cross-linking, and causes a variety of disorders and diseases (*10*−*12*). The recognition of the detriments *and* of the benefits (*13*) of nitrosation increases the complexity of nitrosation toxicology. Hence, a more detailed and quantitative understanding is required of nitrosation in biological environments, and recent studies quantified some nitrosation reagents and products. Wink et al. (*14*) quantified NO production and nitrosation by N_2O_3 using 2,3-diaminonaphthalene (DAN) as a marker, and Mirish et al. (*15*) quantified *N*-nitroso compounds (NOC) and their precursors (NOCP) in foods as markers for potential overall nitrosation damage. Specific damage has been quantified for some nitrosating reagents, and this is exemplified by a study of DNA strand breaks by *N*-nitrosomorpholine (NMOR) in single cells by Robichova and Slamenova (*16*) and by the quantification of the products of DNA base deamination under biologically relevant conditions of NO exposure by Dedon et al. (*17*). In this context, we discuss the suitability of oxanosine as a marker for nucleoside nitrosation.

The main products of nitrosation of derivatives of the DNA bases guanine, adenine, and cytosine are the corresponding derivatives of xanthine, inosine, and uracil, respectively, and they participate in normal cell metabolism irrespective of any possible additional formation by nitrosation (Figure 1). The nitrosation of guanine derivative **1** stands out because its nitrosation forms, aside from the xanthine derivatives **2**, significant amounts of a second type of product, the oxanine derivatives **3**. Suzuki et al. isolated 2′-deoxyoxanosine **3d** as a product of the nitrosation of 2′-deoxyguanosine **1d**, oligodeoxynucleotide (dTGTT), and calf thymus DNA with nitrous acid, HNO_2, and nitric oxide, NO (*18*). Nitrosative deamination of guanosine **1r** yields **3r** in complete analogy.

Oxanosine, 5-amino-3-*β*-(D-ribofuranosyl)-3*H*-imidazo-[4,5-*d*][1,3]oxazine-7-one (**3r**, Figure 1), was isolated as a new antibiotic in 1981 from *Streptomyces capreolus* MG265-CF3, and its structure was determined (*19*, *20*). Oxanosine inhibits the growth of *HeLa* cells in vitro, shows antibacterial activity against *Escherichia coli* K-12,

[§] Department of Chemistry.
[‡] Department of Biochemistry.
* To whom correspondence should be addressed. E-mails: (R.G.) glaserr@missouri.edu; (P.T.) tiptonp@missouri.edu.

10.1021/tx050232h CCC: $30.25
Published on Web 11/09/2005

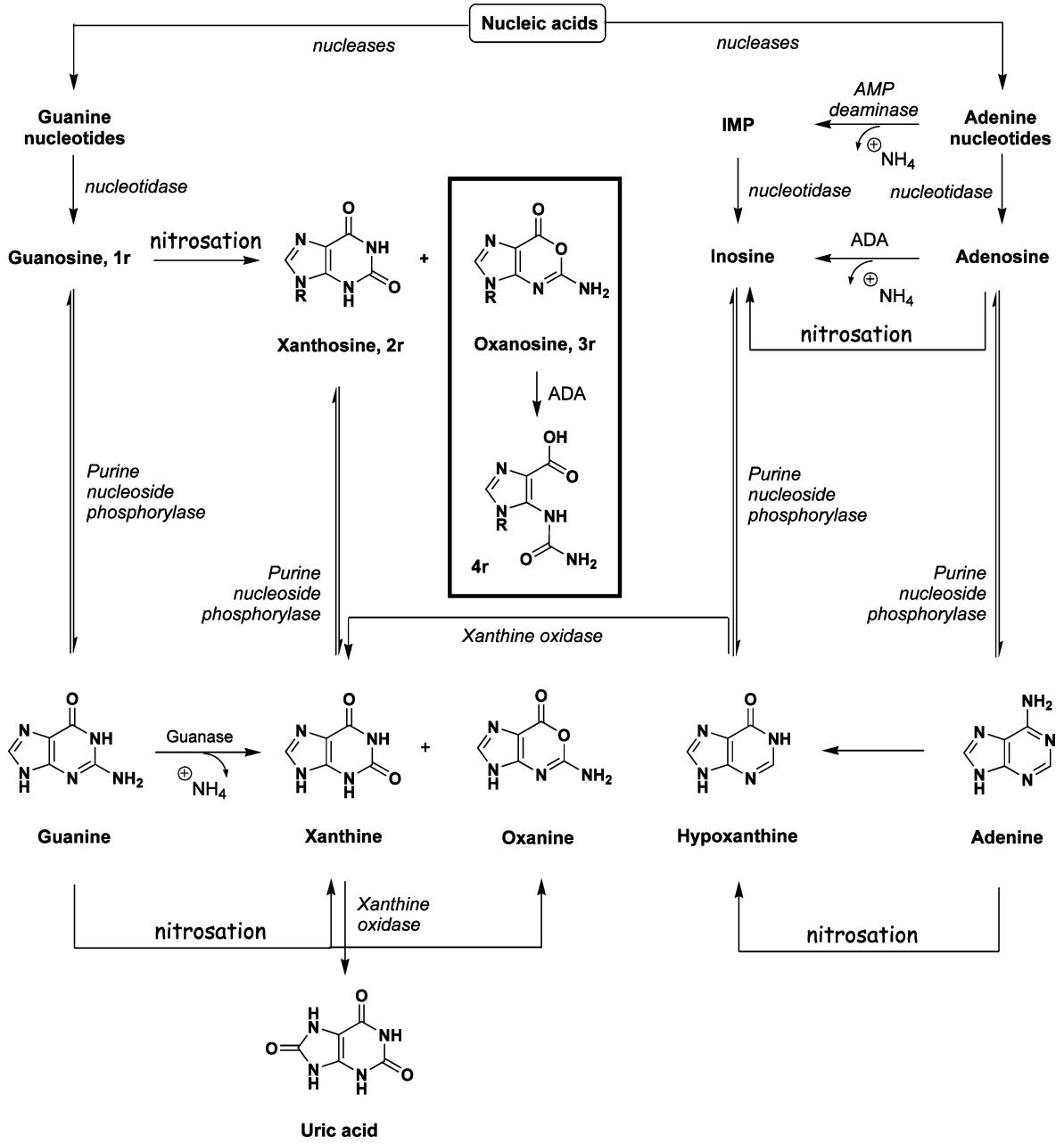

Figure 1. Purine metabolism and nitrosative deamination.

and suppresses the growth of L-1210 leukemia in mice (*19*−*21*). Studies of rat kidney cells infected with mutant *Rous sarcoma* virus (*22*) showed oxanosine to be more cytotoxic to tumor cells than to normal cells, and oxanosine also induced reversion toward the normal phenotype of K-*ras*-transformed rat kidney cells (*23*). There have not been any reports on the presence, the endogenous synthesis, or any physiological function of oxanine derivatives in healthy cells. The presence or absence of oxanine derivatives **3** might thus recommend itself as a suitable measure for nitrosative deamination of guanines **1** and, in a broader sense, as a physiological or toxicological marker of overall nitrosation activity.

We present here the results of a study of the ADA-catalyzed hydrolyses of **3r** to **4r** and of **3d** to **4d** and **4h** (Figure 2). The reaction was studied for another reason, and its outcome was unexpected. We found that ADA promotes the lactone hydrolysis of oxanosine to 1-β-(D-ribo-furanosyl)-5-ureido-1*H*-imidazole-4-carboxylic acid **4r**. ADA also catalyzes the hydrolysis of 2′-deoxyoxanosine **3d** under these conditions to 1-β-(D-2′-deoxyribofuranosyl)-5-ureido-1*H*-imidazole-4-carboxylic acid **4d**. In contrast to **4r**, **4d** easily undergoes deglycation to 4,5-ureido-1*H*-imidazole-4-carboxylic acid **4h** (after its enzymatic formation and release). The study of the ADA-catalyzed hydrolysis of **3d** in (^{18}O)water and of the ADA-catalyzed hydrolysis of **3r** clarified that a lactone hydrolysis was taking place. The products were separated by liquid chromatography and identified and characterized by mass spectrometry and NMR spectroscopy. The known mechanism of action of ADA provides a rationale for the lactone-opening. The Michaelis−Menten parameters for **3r** and **3d** are reported. Implications are discussed for toxicological studies of nitrosative deamination of nucleosides and nucleotides.

Materials and Methods

Materials. Guanosine and 2′-deoxyguanosine (**1r** and **1d**) were purchased from Sigma (purity > 99%) and used without further purification. Adenosine deaminase (calf intestine) was

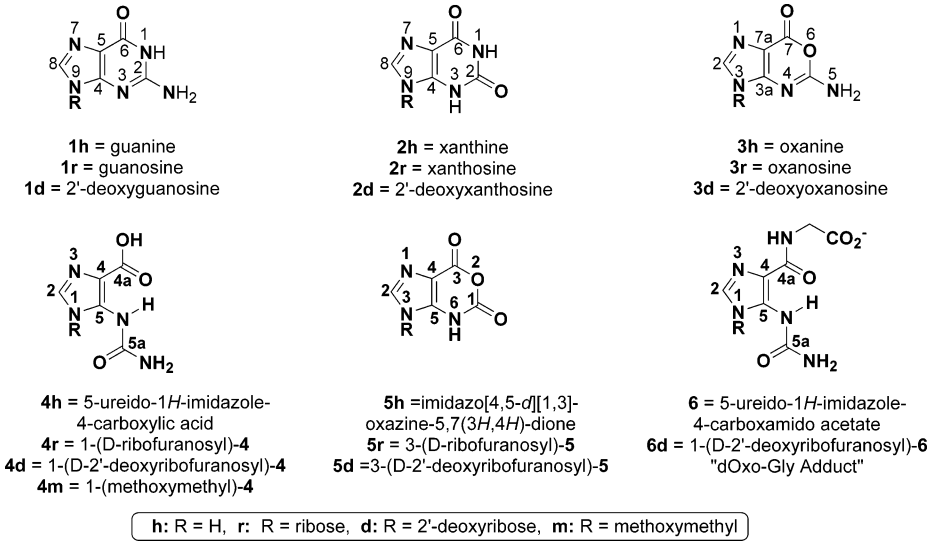

Figure 2. Nitrosative deamination of guanines **1** has been known to form xanthines **2** and oxanines **3**. It has been found now that ADA catalyzes the hydrolysis of oxanosines **3** to compounds **4**. Heterocycles are numbered, and letters specify the R-group. Note that the IUPAC numberings of purine and oxanine derivatives differ.

purchased from Boehringer-Mannheim in solution of 50% glycerol (v/v) and 10 mM potassium phosphate, specific activity 200 units/mg at 25 °C with adenosine as substrate (1 unit ADA activity is the amount of enzyme that produces 1 μmol of inosine per minute). ^{18}O-Water was purchased from Isotech Isotopes Inc. in 97.6% enrichment. HPLC grade acetonitrile was bought from Fisher. The 0.1 M triethylammonium acetate buffer was prepared from glacial acetic acid and triethylamine, filtered through 0.45 μm filter paper under reduced pressure, and sonicated for 15 min before use. Triethylamine was purchased from Acros Organics and purified by distillation over calcium hydride. Distilled water was filtered through a 0.45 μm filter paper under reduced pressure and sonicated for 15 min before use in HPLC.

Syntheses of Oxanosines 3r and 3d by Nitrosation of Guanosines 1r and 1d. Compounds **3r** and **3d** were synthesized by the method of Suzuki et al. (*18*). Compound **1r** (12.5 mM) was incubated at 37 °C with $NaNO_2$ (124.9 mM) in 4 mL of sodium acetate buffer (3 N, pH = 3.7) for 20−24 h to ensure that almost all **1r** had reacted. HPLC analysis of the reaction mixture showed the formations of **2r** (t_R = 9.7) and **3r** (t_R = 13.5). Similarly, **1d** (12.5 mM) was incubated at 37 °C with $NaNO_2$ (124.9 mM) in 4 mL of sodium acetate buffer (3 N, pH = 3.7). HPLC analysis showed the formations of xanthine **2h** (t_R = 7.5), 2′-deoxyxanthosine **2d** (t_R = 9.7), and 2′-deoxyoxanosine **3d** (t_R = 13.5). All HPLC assignments were confirmed by LC/MS analysis. The oxanosines **3r** and **3d** were separated and purified by preparative RP-HPLC and dried by lyophilization.

ADA-Catalyzed Hydrolyses of 3r and 3d in (^{18}O)Water. A 50 mM sodium phosphate buffer (pH = 7.4) was prepared with $H_2{}^{18}O$. Oxanosine **3r** or **3d** was dissolved in the labeled buffer, 60 μL (120 μg, 24 units) ADA was added, and the reaction solution was monitored by HPLC and LC/MS.

RP-HPLC Analyses and Preparations. The RP-HPLC analyses were performed on a Shimadzu LC system that consisted of a LC-10AT*vp* pumping system, CTO-10A*vp* column oven (25 °C), and a SPD-M10A*vp* photodiode array detector. The samples were injected with a SIL 10A autosampler, and the initial mobile phase was 100% 0.1 M triethylammonium acetate buffer. Acetonitrile was mixed into the mobile phase in such a way as to increase the acetonitrile concentration linearly from 0 to 10% over 16 min. For analytical purposes, a Supelcosil octadecylsilane column (2.5 cm × 4.6 mm i.d., 5 μm particle size) was used, and the flow rate was 1 mL/min. The volume of sample injected was 10 μL. For semipreparative work, a Supelcosil octadecylsilane column (25 cm × 10 mm i.d., 5 μm particle size) was used with a flow rate of 4.73 mL/min. The volume of the sample injected was 142 μL. The samples were kept at −5 °C during HPLC analysis to prevent decomposition.

LC/MS Analyses. The LC component consisted of a Finnigan P4000 pump, a AS3000 autosampler, and a UV6000 LP detector. The mobile phase initially was 0.1 M triethylammonium acetate buffer, and acetonitrile was mixed in linearly and up to 10% over 16 min. The flow rate was 1 mL/min, and the injection volumes were 20 μL. The separations were carried out on a Supelcosil octadecylsilane column (2.5 cm × 4.6 mm i.d., 5 μm particle size). The LC was coupled to a TSQ 7000 triple-quadrupole mass spectrometer (Thermoquest, San Jose, CA) which was operated in the negative ion atmospheric pressure chemical ionization (APCI) mode for the analysis. The temperature of the heated capillary was 350 °C.

NMR Spectroscopy. The ^{1}H and ^{13}C NMR spectra were recorded on a Bruker Avance DRX500 spectrometer equipped with a 5 mm broadband probe in DMSO-d_6 (^{1}H) or CD_3OD (^{13}C). A 30° excitation pulse was applied to record ^{1}H and ^{13}C NMR spectra. All ^{13}C NMR spectra were acquired with broadband ^{1}H decoupling. Repetition times were 3.78 (^{1}H) and 1.82 s (^{13}C). All the ^{1}H NMR spectra are the result of the accumulation of 32 scans, while 20 000−40 000 scans were accumulated for ^{13}C NMR spectra depending on sample concentration. Line-broadenings of 0.2 (^{1}H) or 1 Hz (^{13}C) were applied. The methanol signals at $\delta(^1H)$ = 3.30 and $\delta(^{13}C)$ = 49.0 ppm and the DMSO signal at $\delta(^1H)$ = 2.49 ppm served as internal standards. The isotopic shift is reported in parts per million and hertz. Peak assignments were based on literature (*24*, *25*). DMSO-d_6 was used for the measurements of the ^{1}H NMR spectra.

We determined the position of the label via the ^{18}O-isotopic shifts in the ^{13}C NMR spectra (*26*). The ^{18}O-isotopic shifts of ^{13}C NMR signals have been studied for several functional groups, and their magnitudes vary in ways that are not easily predictable (*27*). These ^{18}O isotope shifts are only a few hertz, and the choice of solvent was critical for their measurement. The carbonyl peaks in the ^{13}C NMR spectra of **3r** and **4r** were difficult to measure in DMSO because of the solvent's high viscosity; the signals could only be recorded with longer relaxation times (6.65 s) but were then too broad (30−40 Hz). Methanol-d_4 was found to be the ideal solvent to measure the isotopic shifts providing very sharp peaks with widths of only 2−4 Hz.

Computational Methods. Structures of **3h**, **4h**, and **4m** (Figure 8) were optimized with the B3LYP implementation of hybrid density functional theory (*28*) with the program Gaussian03 (*29*). The fully polarized valence triple-ζ basis set 6-311G**

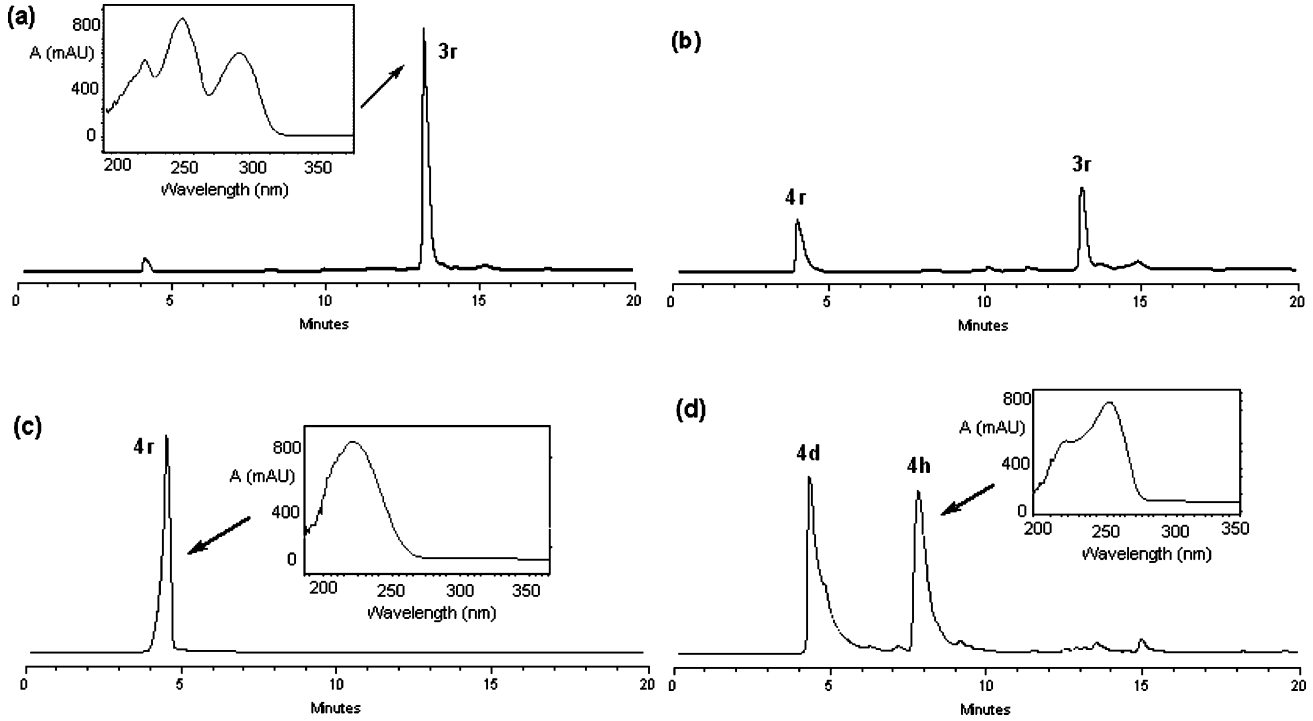

Figure 3. RP-HPLC chromatograms of the ADA-catalyzed hydrolyses of **3r** and **3d**: (a) within 30 s of ADA addition to **3r** (inset: UV spectrum of **3r**), (b) as the reaction of **3r** to **4r** progressed, and (c) after completion (inset: UV spectrum of **4r**). The reaction of **3d** is similar, except for the product deglycation; (d) **4d** and **4h** (inset: UV spectrum of **4h**).

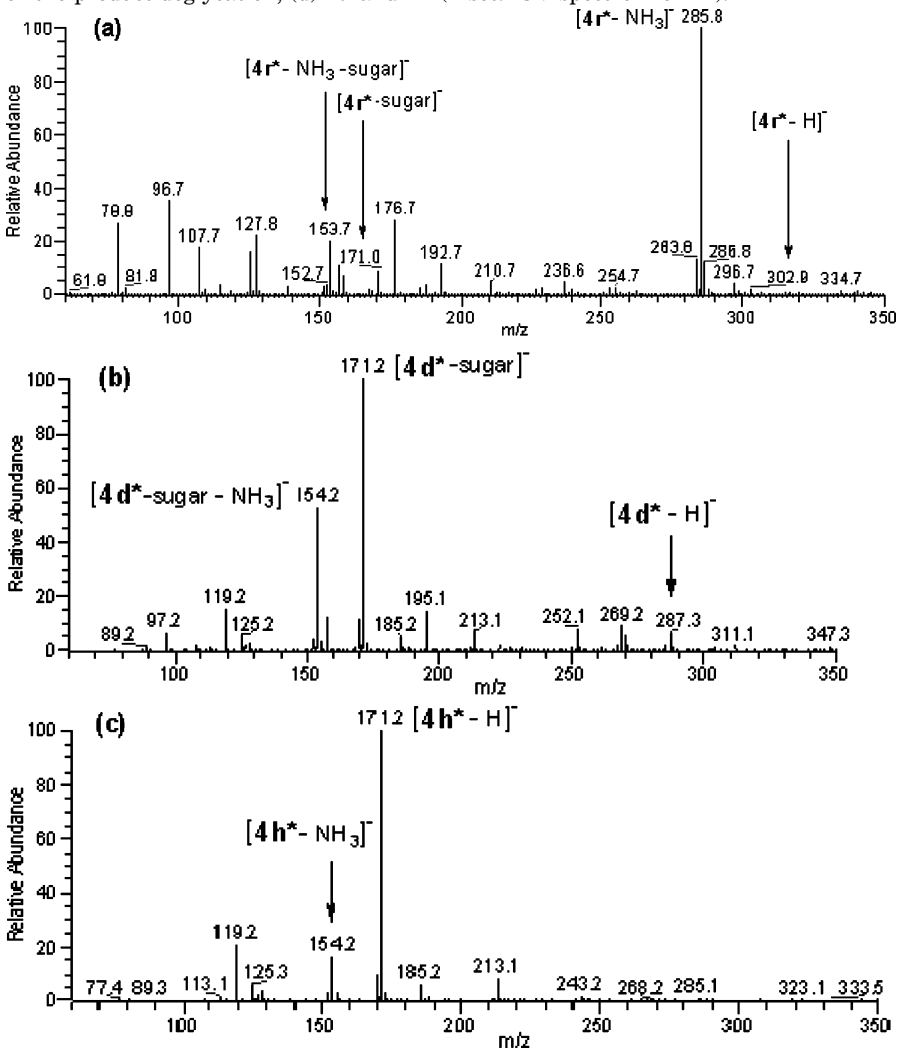

Figure 4. LC/MS spectra of the ADA-catalyzed hydrolyses of **3r** and **3d** with (^{18}O)water. Product **4r** (t_R = 4.0 min, panel a) of the ADA-catalyzed reaction of **3r**. Products **4d** (t_R = 4.4 min, panel b) and **4h** (t_R = 8.2 min, panel c) of the ADA-catalyzed reaction of **3d**.

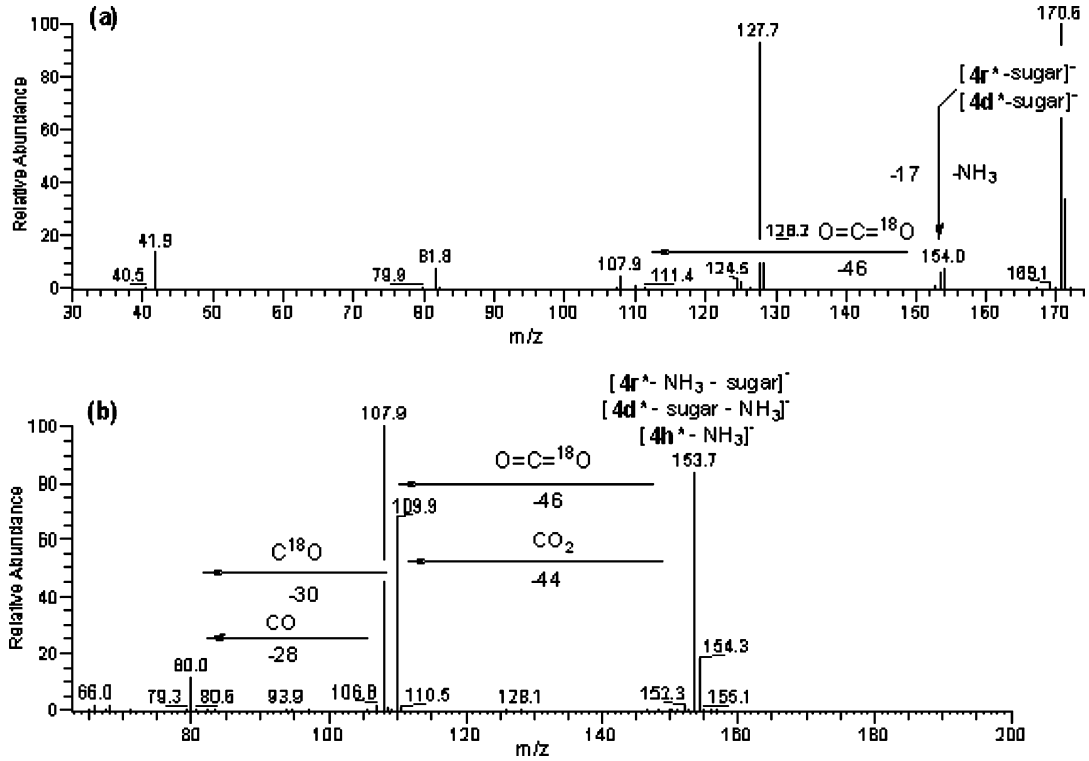

Figure 5. (a) The MS/MS spectrum of ion $[\mathbf{4h}^*-H]^-$ with $m/z = 171$, formed directly from **4h*** or by deglycation of **4r*** or **4d***, features fragment peaks at $m/z = 154.0$ and $m/z = 127.7$. (b) The MS/MS spectrum of ion $m/z = 154$ shows further fragmentation releasing first ^{18}OCO and then CO or first CO_2 and then ^{18}OC.

was employed for all optimizations (= basis set A) (*30*). Vibrational frequency analyses were carried out at the level of optimization to confirm that a stationary structure indeed had been located and to confirm the character of the stationary structure (e.g., minimum, no imaginary modes). The Gauge-Independent Atomic Orbital (GIAO) method is a proven, efficient, and accurate method for the calculation of NMR shielding tensors (*31*) and GIAO-NMR calculations were carried out in conjunction with the B3LYP method. The NMR calculations employed basis set A and also Dunning's correlation-consistent polarized valence triple-ζ and quadruple-ζ basis sets cc-pVTZ (= basis set B) and cc-pVQZ (= basis set C), respectively (*32*). NMR calculations were carried out for the isolated molecule as well as for model-solvated molecules. The solvation calculations employed the Polarized Continuum Model (PCM, *33*) to simulate methanol ($\epsilon = 32.63$) and DMSO ($\epsilon = 46.7$).

Kinetic Analyses of the ADA-Catalyzed Hydrolysis of Oxanosine 3r and Adenosine. Kinetic analyses of the ADA-catalyzed hydrolyses of **3r** and adenosine **7r** were performed with a Hewlett-Packard diode array spectrophotometer 8452A equipped with T-control (Peltier cell holder, 220−400 nm; scanning time = 40 min, 1 scan per second). Absorption spectra were collected at 37 °C, and the change in absorbance at 300 nm was recorded to monitor ADA activity as a function of the concentration of **3r** or **7r**, using $\epsilon_{300}(\mathbf{3r}) = 3800\ M^{-1}\ cm^{-1}$ (cf. $\epsilon_{260}(\mathbf{3r}) = 5100\ M^{-1}\ cm^{-1}$ (*18*)) and $\epsilon_{260}(\mathbf{7r}) = 15\,400\ M^{-1}\ cm^{-1}$ (*18*). Assays were carried out in 50 μM sodium phosphate buffer (pH = 7.4). Activities were measured over at least 15 concentrations of **3r** and **7r** (0.1−3 K_M), and cuvettes with 0.2 and 1 cm path lengths were used to widen the range. ADA concentrations were kept constant (**3r**, 1.5 μM; **7r**, 0.75 nM), and each assay was repeated at least three times. V_{max} values were adjusted to reflect the ADA concentration.

Results

Preparation, Isolation, and UV/Vis Analysis of 4. Samples of 25 mM of oxanosines **3r** and **3d** were incubated with 3 μM ADA in 50 mM sodium phosphate buffer (pH = 7.4) at 37 °C for 5 h. RP-HPLC chromatograms of the ADA-catalyzed hydrolyses of **3** are shown in Figure 3. The substrates **3r** and **3d** were completely consumed after 5 h. The products were isolated by semipreparative RP-HPLC for structural analysis.

Substrate **3r** reacted cleanly to **4r**; Figure 3a was recorded just after ADA addition ($t_R(\mathbf{3r}) = 13.5$ min), and panels b and c of Figure 3 were recorded during and after completion of the enzymatic reaction ($t_R(\mathbf{4r}) = 4$ min, $\lambda_{max} = 228$ nm for **4r**). Substrate **3d** reacted cleanly to **4d** in the same way, but in this case, deglycation of **4d** is significant (after its enzymatic formation and release); about half of product **4d** (Figure 3d, $t_R(\mathbf{4d}) = 4.4$ min; $\lambda_{max} = 228$ nm for **4d**) was converted to **4h** (Figure 3d, $t_R(\mathbf{4d}) = 8.2$ min, $\lambda_{max} = 257$ nm) by the time the enzymatic reaction was complete. With regard to t_R and absorbance, **4r** and **4d** resemble adduct **6** (*25*).

Structure Assignment via Mass-Spectrometry and ^{18}O-Labeling. The negative ion APCI-LC/MS spectra (Figure 4) show the products of the ADA-catalyzed hydrolyses of **3r** and **3d** with (^{18}O)water and prove that one ^{18}O-label is incorporated in **4r***, **4d***, and **4h***. The spectrum of **4r*** (Figure 4a) shows signals at *m/z* values of 302.9 (**4r***-H), 285.8 (**4r***-NH_3), 171 (**4r***-sugar), and 153.7 (**4r***-NH_3-sugar). The spectrum of **4d** (Figure 4b) features only a very weak pseudomolecular ion peak at $m/z = 287.3$ (**4d***-H) and strong peaks with *m/z* values of 171.2 (**4d***-sugar) and 154.2 (**4d***-sugar-NH_3). The deglycation product **4h** with $m/z = 171$ was identified by its negative ion APCI-LC/MS/MS spectrum (Figure 4c).

The negative ion APCI-LC/MS/MS spectra of **4r*** and **4d*** are shown in Figure 5. The major fragmentations of ion $m/z = 171$ (Figure 5a) involve deglycation to $m/z = 154$ and HNCO loss to $m/z = 128$. The MS/MS spectrum of ion $m/z = 154$ provides compelling evidence for the

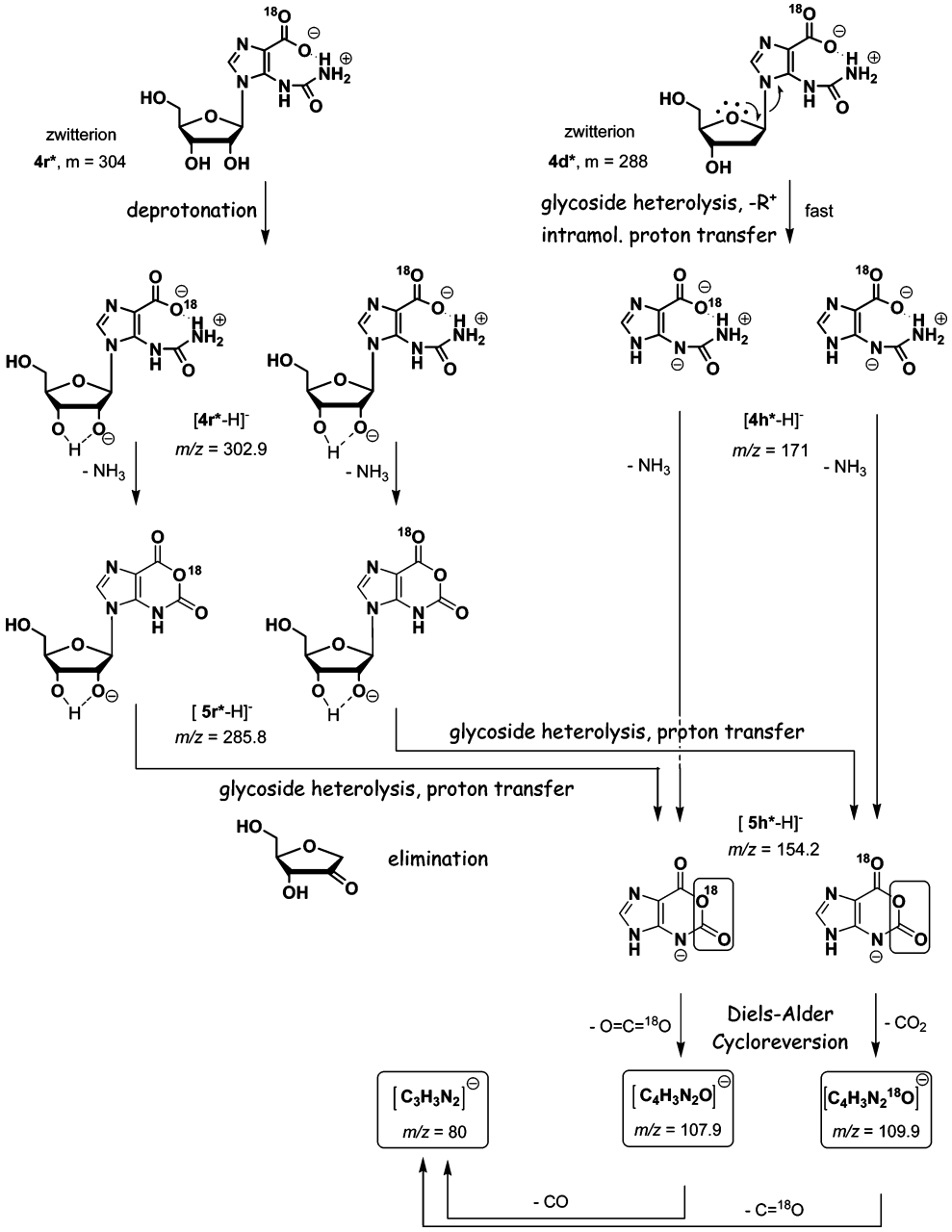

Figure 6. Proposed major fragmentation paths of **4r***, **4d***, and **4h***.

formations of daughter ions by initial elimination of either ^{18}O-labeled or unlabeled CO_2 via Diels−Alder cycloreversion followed by elimination of either unlabeled or ^{18}O-labeled CO, respectively (Figure 5b).

The MS spectra are consistent with the major fragmentation paths of **4r***, **4d***, and **4h*** shown in Figure 6. The −COOH···NH_2CO− hydrogen bond in **4** is prone to form the zwitterion −COO^-···H^+NH_2CO− of **4**, and this explains the propensity for facile NH_3 loss. We show the zwitterionic structure in Figure 6 to stress its latency. Because of the equilibrium between **4**(−COOH···NH_2CO−) and **4**(−COO^-···H^+NH_2CO−), **4** does not contain an ammonium ion as such. The most acidic hydrogen in **4r** is that of the 2′-hydroxyl group ($pK_a \approx 13.0 \pm 0.5$, *34*), and this hydroxyl group is deprotonated to form the ion [**4r**−H]$^-$ in which the oxyanion is stabilized by intramolecular hydrogen bonding. In the absence of the 2-hydroxy group, the ion [**4d**−H]$^-$ is not formed and ion [**4h**−H]$^-$ is formed instead. The facile deglycation of 2′-deoxyribosides (Figure 4b) has precedent in negative ion MS (*35*). The sequence of NH_3 elimination and deglycation differ for the riboside and the 2′-deoxyriboside, and they feature different mechanisms of glycoside heterolysis. The riboside **4r*** deprotonates, then eliminates NH_3 ($m/z = 285.8$), and finally eliminates the ribose ($m/z = 154$) as neutral dihydrofuran-3(2*H*)-one. In contrast, 2′-deoxyriboside **4d*** initially undergoes *N*-glycosidic bond cleavage ($m/z = 170.6$) and then NH_3 elimination ($m/z = 154$). Both paths eventually lead to ion [**5h**−H]$^-$, and the structure of this anion shown in Figure 6 reflects the much higher acidity of 2-pyridone ($pK_a = 11.6$, *36*) and its derivatives compared to imidazole.

Structure Confirmation via NMR Spectroscopy. The ^{1}H NMR spectrum of **4r** (DMSO-d_6, 25 °C, Supporting Information) exhibits a set of signals for the ribose moiety of **4r** and the NH_2 protons: δ 8.13 (s, 1H, NHCONH$_2$), 7.89 (s, 1H, H-2), 6.29 (s, 2H, NH$_2$), 5.5 (d, H-1′), 4.12 (t, H-2′), 4.04 (t, H-3′), 3.84 (m, ABX, H-4′), 3.65 (m, ABX, 2H, H-5′,5″). The ^{1}H NMR spectrum of **4d**

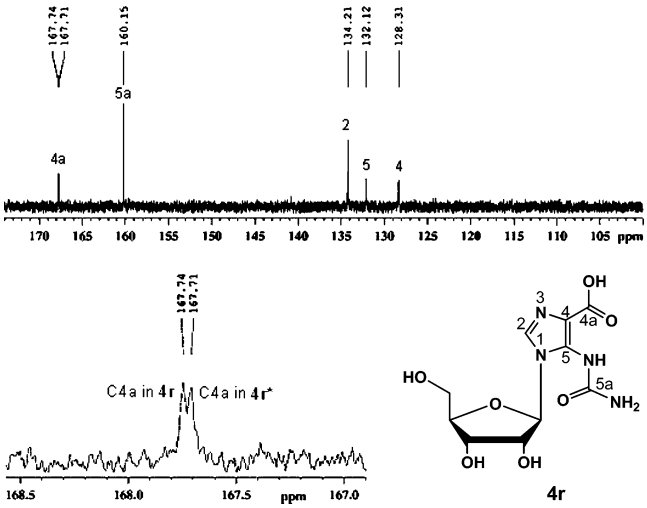

Figure 7. The ^{13}C NMR spectrum of **4r** recorded in CD_3OD (above, ribose signals not shown). The ^{13}C NMR spectrum of a mixture of **4r** and (^{18}O)-labeled **4r*** shows an ^{18}O-isotopic shift of 15.0 Hz for the C4a atom.

showed the same signals, and both are identical with **6** (*25*) and with the ribose moiety for nucleosides (*24*, *25*). The ^1H NMR spectrum of **4r** in methanol-d_4 did not show any signals for the exchangeable protons ($NHCONH_2$). The ^{13}C NMR spectrum of unlabeled **4r** (CD_3OD) was recorded (Figure 7) and assigned as follows: δ 167.74 (COOH, C4a), 160.15 ($NHCONH_2$, C5a), 134.21 (C2, DEPT), 132.12 (C5), 128.31 (C4), 90.47 (C1′), 85.99 (C4′), 77.25 (C2′), 73.86 (C3′), 64.34 (C5′). The ^{13}C NMR spectrum of unlabeled **4d** (CD_3OD) was recorded and assigned: 165.24 (COOH, C4a), 156.52 ($NHCONH_2$, C5a), 132.73 (C5), 132.10 (C2, DEPT), 123.66 (C4), 87.62 (C4′), 84.22 (C1′), 70.58 (C3′), 61.58 (C5′), 40.84 (C2′). These spectra and that of **6** (*25*) are very similar.

To detect any ^{18}O-isotopic shifts on the ^{13}C NMR signals of **4r**, the ^{13}C NMR spectrum of unlabeled **4r** was recorded first and a second spectrum was recorded after addition of a similar amount of ^{18}O-labeled **4r***. An ^{18}O-isotopic shift of 15.0 Hz (Figure 7) was measured for C4a (COOH); hence, C4a was attached to one ^{16}O and one ^{18}O, and the ^{18}O incorporation occurred exclusively at C4a.

Computed Structures and NMR Chemical Shifts. The structures of **3h**, **4h**, and **4m** were determined at the B3LYP/6-311G** level, and several conformers and tautomers were examined for **4h** and **4m**. The structures shown in Figure 8 are greatly preferred, and they share a number of features: (a) The COOH group is oriented such that the carbonyl-O is available as a hydrogen bond acceptor; (b) the conformation of the C−NH bond positions the urea NH group for intramolecular hydrogen-bonding to the acid-carbonyl; (c) the NH−CO conformation is such that the urea-carbonyl is proximate to the imidazole; and (d) the acid-hydroxyl group is oriented toward the imidazole-N. The *Z*-conformation about C−NH is required for the intramolecular urea−NH···OC−acid hydrogen bond. The *Z*-conformation about the NH−CO bond allows for an additional intramolecular NH···OC hydrogen bond between the urea−carbonyl and the imidazole−NH. The latter would not occur in the nucleoside, and **4m** was therefore examined as a small nucleoside model. The general features of **4h** persist in the nucleoside model, but torsional distortions occur in **4m**. GIAO-NMR chemical shifts were computed based on the B3LYP/6-311G** structures, with the B3LYP and PCM-B3LYP methods, and using basis sets A−C. The results (provided as Supporting Information) show that solvent effects were marginal and the calculated chemical shifts for **4h** and **4m** corroborate the structure assignments for **4r** and **4d**.

Michaelis−Menten Analysis. The K_M and V_{max} values were measured for adenosine and oxanosine (Table 1). Several measurements were reported of the Michaelis−Menten constant for adenosine and 2′-deoxyadenosine, respectively, and the literature values are $K_M = 50$ μM (*37*, 1967), 31 μM (*38*, 1969), 45 μM (*39*, 2001), and 38 μM (*40*, 2003) for adenosine, and $K_M = 22$ μM (*38*, 1969) and 34 μM (*39*, 2001) for 2′-deoxyadenosine. Our result for adenosine is in good agreement with the literature data. The Michaelis−Menten constant of K_M

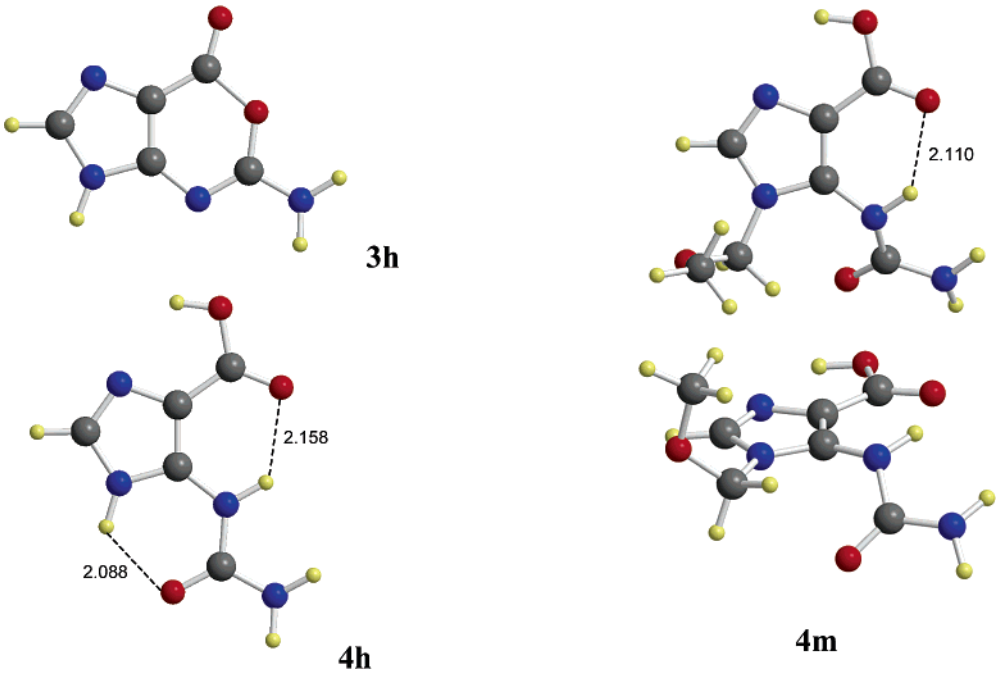

Figure 8. Molecular models of **3h**, **4h**, and **4m** determined by ab initio calculations.

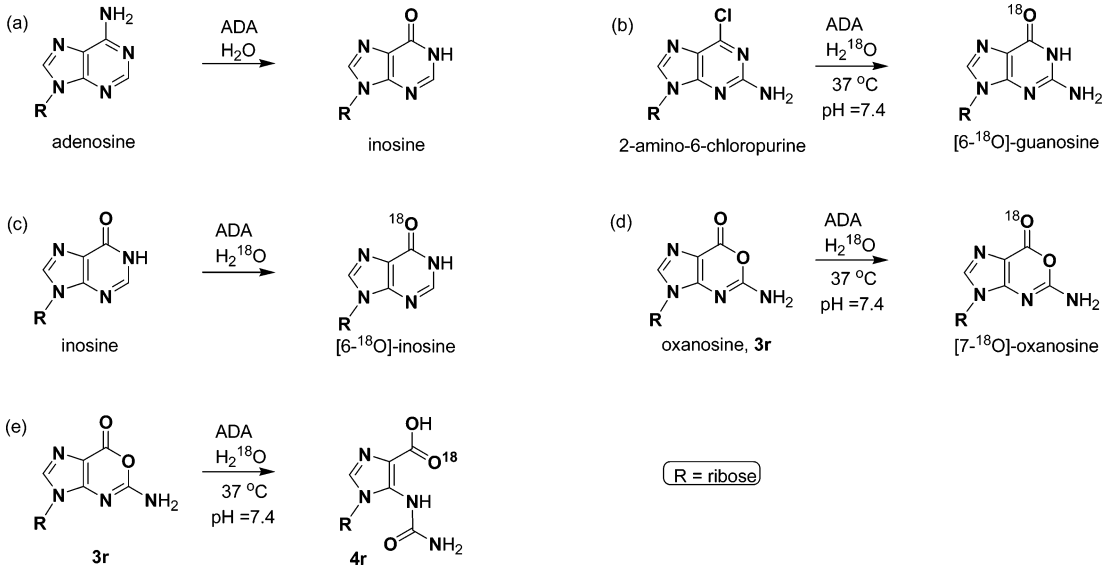

Figure 9. (a) Adenosine is converted to inosine when treated with ADA. (b) 2-Amino-6-chloropurine is converted to [6-^{18}O]-**1r** when treated with ADA. (c) ADA-catalyzed exchange of ^{18}O into inosine. (d) Expected exchange of C7 carbonyl oxygen of **3r** in ADA-catalyzed reaction of **3r** in (^{18}O)water. (e) Actual ADA-catalyzed reaction of **3r** in (^{18}O)water.

Table 1. Substrate Selectivity of ADA[a,b]

compound	wavelength (nm)	K_M (μM)	V_{max} (μmol/s)	*rel.* V_{max}[a] (%)	V_{max}/K_M
adenosine	260	46 (±8)	0.133	100	2
2′-deoxyadenosine[c]	260	28 (±6)	0.124	93	3.3
oxanosine	300	1040 (±170)	4.8	1.8	0.002

[a] *Rel.* $V_{max} = (c_{ADA}/V_{max})^{Adenosine} \cdot (V_{max}/c_{ADA})^{Oxanosine}$. [b] In the present case, $2000 \cdot c_{ADA}{}^{Adenosine} = c_{ADA}{}^{Oxanosine}$. [c] Based on refs *38* and *39*.

= 1040 (±170) μM was measured for oxanosine. The data in Table 1 show only a minor difference in the substrate activities of **7r** and **7d** with ADA. The same is likely to be true for **3r** and **3d** and justifies why only **3r** was measured.

Discussion

Motivation, Expectation, and Serendipity. The ^{18}O-labeling studies of nitrosative deamination of guanosine **1r** established the formation of oxanosine **3r** via the intermediates of ribose derivatives of 5-cyanoimino-4-oxomethylene-4,5-dihydroimidazole and 5-cyanoamino-4-imidazolecarboxylic acid (*41*). These experimental results fully corroborated the prediction of 5-cyanoimino-4-oxomethylene-4,5-dihydroimidazole as the primary product of dediazoniation of guaninediazonium ion with concomitant ring-opening (*42*). The intermediates are consistent with the electronic structures of 5-cyanoimino-4-oxomethylene-4,5-dihydroimidazoles and their N-protonated derivatives and justify the chemical syntheses and study of the cyanoamino intermediates (*43*, *44*).

The labeling experiments employed adenosine deaminase (aka adenosine aminohydrolase, ADA, EC 3.5.4.4) for the synthesis of a labeled substrate. ADA is important in purine metabolism, and its primary function is the NH_2/OH-replacement at C6 of adenosine and 2′-deoxyadenosine to form their respective inosine derivatives and NH_3 at about neutral pH (*38*, *45*, *46*). Substitution of C8 by S or O and presence of ribose as a substituent on either the positions 3 or 9 result in large rate enhancements (*38*). ADA from calf intestinal mucosa is known for its ability to hydrolyze several chemically unrelated C6-substituents of purine ribonucleosides (*38*). Hence, we attempted the ADA-catalyzed synthesis of [6-^{18}O]-**1r**, and indeed, this reaction (Figure 9b) was successful and gave [6-^{18}O]-**1r** in 90% yield within hours (*41*).

ADA also can exchange the C6 carbonyl oxygen of hypoxanthine (*47*, *48*) as illustrated in Figure 9c and, on the basis of this knowledge, the question was explored as to whether this catalysis could be exploited to replace the carbonyl oxygen of **3r**. [7-^{18}O]Oxanosine is a known product of nitrosative guanosine deamination in (^{18}O)-water, and a preparation of isotopically pure [7-^{18}O]-**3r** was sought (*41*). Yet, the ADA-catalyzed reaction of **3r** with ^{18}O-labeled water did not form [7-^{18}O]-**3r** (Figure 9d), and instead, 1-β-(D-ribofuranosyl)-5-ureido-1*H*-imidazole-4-carboxylic acid, **4r**, was formed (Figure 9e).

Mechanisms of ADA-Catalysis. The hydrolysis of **3** to **4** can be explained in a manner that is consistent with the known mode of action of ADA for adenosine (*49*); see Figure 10. At the same time, there is a significant difference between the accomplishment of the "usual" substitution at C6 (addition to the exocyclic bond) and the "lactone hydrolysis" (addition to the endocyclic double bond), and this is illustrated in Figure 11.

The mechanism of ADA-catalysis of adenosine deamination (Figure 10) begins with the positioning and activating of water by hydrogen-bonding to Asp-295 and His-238 and O-coordination to the Zn^{2+} ion. The proton affinity of His-238 (PA = 350 kcal·mol^{-1}, *50*) greatly exceeds that of a primary amine (PA ≈ 207−223 kcal·mol^{-1}, *51*) and water heterolysis leads to the protonation of the former. The hydroxide begins the nucleophilic water addition to the adenosine C6=N1 bond by its addition to C6, and Glu-217 protonates adenosine-N1 to complete the water addition (Figure 10). The elimination from the tetrahedral intermediate requires proton catalysis, and this catalysis is provided by the protonated His-238. Proton transfer from protonated His-239 to the NH_2-group releases ammonia, and the return of the N1-proton to the carboxylate of Glu-217 completes the H_2O/NH_3 replacement (*52*).

Oxanosine fits well into the active site; it is positioned by hydrogen bonds to N3 and N7 as with adenosine, and

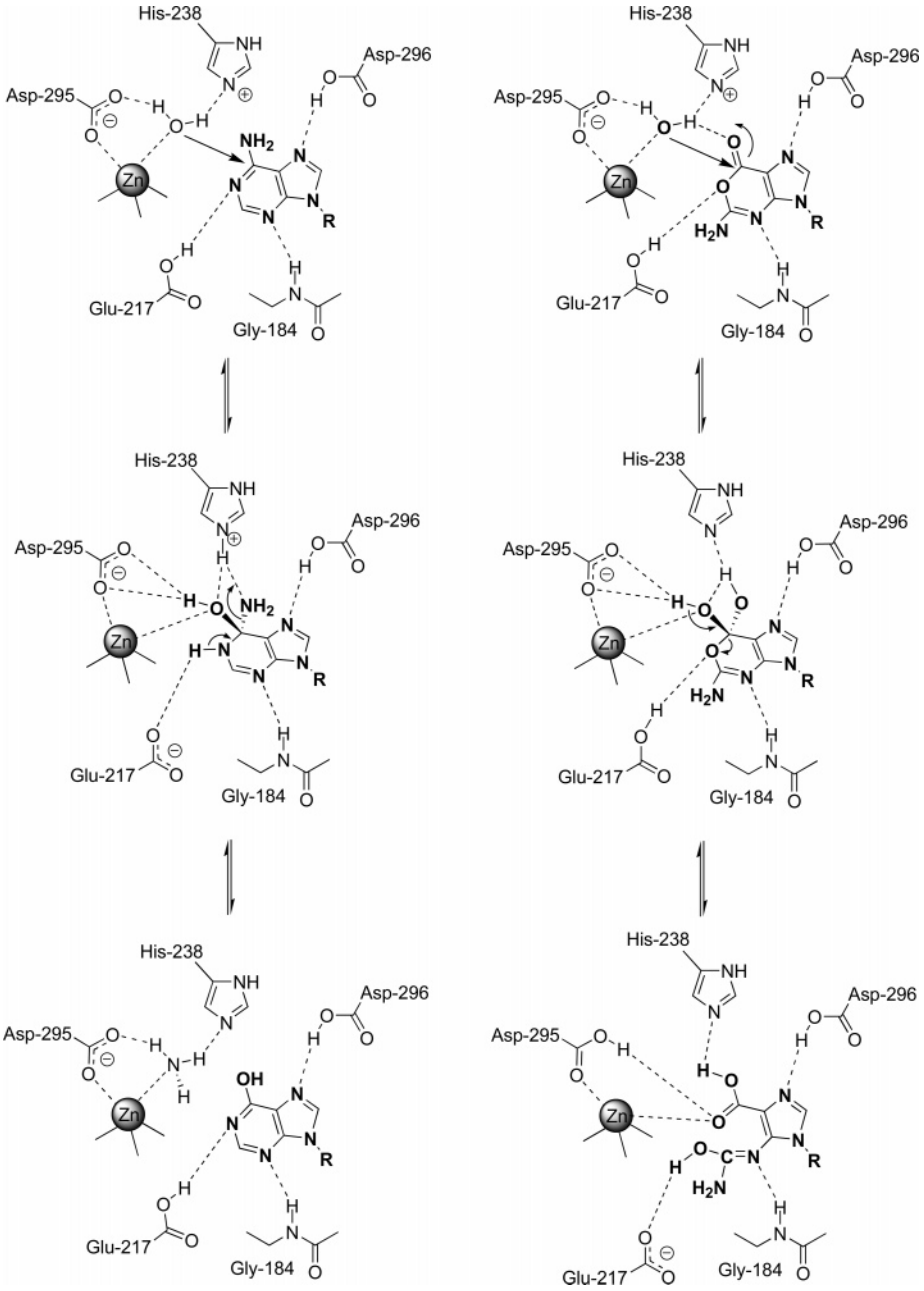

Figure 10. The mechanism for the ADA-catalyzed deamination of adenosine is shown on the left, and the proposed mechanism on the right provides a rationale for the hydrolysis of **3** to **4**.

its C6═O group takes the place of the C6−NH_2 group of adenosine. The heterolysis of water again protonates His-238 as the hydroxide begins to add to C7. But a significant difference occurs during the process of the hydroxide addition: the carbonyl-oxygen (PA ≈ 154−185 kcal·mol^{-1}, *53*) becomes increasingly negative until its proton affinity exceeds that of His-238, proton transfer from His-238 to the carbonyl-O occurs, and an ester hydrate is formed. The cleavage of the ester hydrate requires acid catalysis, and the protonation of the O6-oxygen by Glu-217 is the *only one option*. Hence, the O6−C7 bond is broken to produce the iminol-tautomer of **4r**.

Glu-217 and His-238 guarantee that (a) an addition to the endocyclic double bond is followed by an elimination that restores the endocyclic bond and that (b) the addition to the exocyclic double bond leads to ring-opening. One proton source is required for the addition, and the other must catalyze the elimination (Figure 11). It is for this limited availability of proton donors that adenosine cannot undergo amidine hydrolysis and that oxanosine cannot undergo C6-substitution.

Implications for Chemical Toxicology. Our experiments demonstrate that oxanosine and 2′-deoxyoxanosine are substrates of adenosine deaminase. The ADA-catalyzed hydrolysis initiates the formation of 1-*β*-(D-ribofuranosyl)-5-ureido-1*H*-imidazole-4-carboxylic acid **4r**, 1-*β*-(D-2′-deoxyribofuranosyl)-5-ureido-1*H*-imidazole-4-carboxylic acid **4d**, and 5-ureido-1*H*-imidazole-4-carboxylic acid **4h**. ADA has a wide phylogenetic distribution, and its amino acid sequence is highly conserved from bacteria to humans (*54*). ADA is found in virtually all human tissues, and the highest levels occur in the lymphoid system such as lymph nodes, spleen, and thymus (*39*). It is ADA's primary function to control **dA**

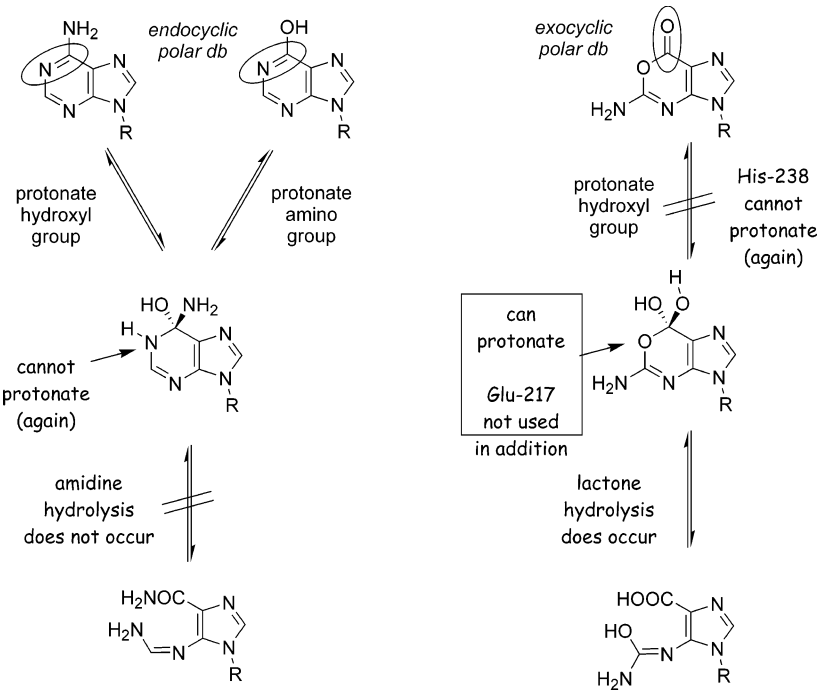

Figure 11. Mechanisms of ADA-catalysis: substitution at C6 by addition to *endocyclic* double bond and elimination vs addition to *exocyclic* double bond and ring-opening elimination.

Table 2. Cellular Concentrations of Nucleosides and Nucleotides

	concentration[a]	
compound	pmol/10^7 cells	μM
GTP (*56*)		449
GDP (*56*)		200
GMP (*56*)		19
ATP (*56*)		4520
ADP (*56*)		1050
AMP (*56*)		186
adenosine (*57*)	11	1.1
2′-deoxyadenosine (*57*)	12	1.2
inosine (*57*)	19	1.9
NO (*17*)		1.3

[a] Conversion from pmol/10^7 cells to μM is based on the approximation of 10^{12} cells per liter, that is, on a typical cell volume of 10^{-12} dm^3 (e.g., length of red blood cell is ca. 10 μm).

levels by converting excess **dA** to inosine which is converted later to hypoxanthine and on to xanthine and uric acid (*55*, Figure 1).

The ubiquity of ADA ensures that oxanosine nucleosides produced anywhere in the body could be converted to **4** by lactone hydrolysis. Whether this conversion actually occurs in biological systems can be assessed on the basis of the data in Tables 1 and 2. The concentrations of the nucleotides are relatively well-established (*56*), and the concentrations of the adenine and guanine nucleotides are listed in Table 2. Cellular concentrations of the nucleosides are less well-established, but accurate data for adenosine, 2′-deoxyadenosine, and inosine were reported recently (*57*): the concentrations are in the micromolar range and about 2 magnitudes smaller that the concentration of the mononucleotide. The concentrations of the **G**-nucleotides are 1 magnitude lower than those of the **A**-nucleotides. It is reasonable to assume that **G**-nucleoside concentrations also are a magnitude lower than **A**-nucleoside concentrations, and there is certainly no reason to assume they are higher than **A**-nucleoside concentrations. The nitric oxide concentrations are micromolar in cells (*17*). If we assume that the **G**-nucleoside concentrations are as high as the **A**-nucleoside concentrations (e.g., 2.2 μM), that only **G**-nucleosides will be deaminated, that all NO is used to deaminate, and that **G**-nucleoside deamination proceeds with a 20% yield of oxanosine nucleosides, then we obtain an upper limit of the concentration of oxanosine nucleosides of about 0.26 μM and realize that the actual concentration of oxanosine nucleosides is likely to be several magnitudes lower. The V_{max}/K_M data of Table 1 show that the lactone hydrolysis of oxanosine is 1000-fold slower than the enzymatic deamination of **A** or **dA**. The combination of nitrosation reagent concentration, relative substrate concentrations, and of the relative reactivities of the substrates shows that the ADA-catalyzed lactone hydrolysis of oxanosine nucleosides will be very slow and essentially negligible in biological system. Hence, the concentration of oxanosine nucleosides indeed presents itself as a suitable and advantageous candidate as a toxicological marker for cellular nitrosation.

The ADA-catalyzed lactone hydrolysis of oxanosines does have implications for studies of nitrosative deamination of nucleosides, nucleotides, and ss- and ds-DNA that are conducted with nonbiological concentrations of substrates and reagents and/or nonbiological concentration ratios of the ADA substrates. The first implication concerns the inadvertent destruction of oxanosine derivatives during workup of nitrosation experiments on nucleotide substrates. To remove the phosphate groups from nucleotides, alkaline phosphatase is generally used and commercial stocks of this enzyme frequently contain small admixtures of ADA (*17*). In those studies where an ADA inhibitor was added (e.g., 8*R*-deoxycoformycin, $K_I = 2.5 \times 10^{-12}$, *58*), it was added to prevent the deamination of *adenosine*. Our results suggest that a specific ADA inhibitor also should be used in the DNA digestion of any deamination experiments of *guanosine* in which oxanosine might play a role (*17*, *59*). Alternatively, controls are required to ensure that the ADA-

catalyzed lactone hydrolysis of oxanosine is in fact slow compared to the DNA digestion. In cases where the ADA-catalyzed lactone hydrolysis of oxanosines does play a significant role, several options present themselves. The consideration of the combined total oxanosines **3** and **4** is one option. Alternatively, one may deliberately *add* ADA to convert all **3** to **4** and employ **4** as the toxicological marker for nitrosative stress.

Acknowledgment. This work was supported by the National Institutes of Health (GM61027). We thank NMR spectroscopist Dr. Wei Wycoff and mass spectrometrist Dr. Nathan Leigh for their assistance.

Supporting Information Available: Four figures showing the UV/vis spectra of the ADA-catalyzed hydrolysis of **3r**, the ^{1}H NMR spectrum of **4r** in DMSO-d_6, and molecular models of conformers and isomers of **4h** and **4m**, a table with B3LYP/6-311G** total energies and thermodynamical data, two tables with calculated chemical shifts, and Cartesian coordinates of optimized structures. This material (13 pages) is available free of charge via the Internet at http://pubs.acs.org.

References

(1) Committee on Nitrite and Alternative Curing Agents in Food (1981) The health effect of nitrate, nitrite, and *N*-nitroso compounds. National Academy Press, Washington, DC.

(2) *Health Assessment Document for Diesel Engine Exhaust.* EPA/600/8-90/057F, U.S. Environmental Protection Agency, National Center for Environmental Assessment, Office of Research and Development, Washington, DC, May 2002.

(3) Korhonen, R., Lahti, A., Kankaanranta, H., and Moilanen, E. (2005) Nitric oxide production and signaling in inflammation. *Curr. Drug Targets: Inflammation Allergy 4*, 471−479.

(4) Guzik, T. J., Korbut, R., and Adamek-Guzik, T. (2003) Nitric oxide and superoxide in inflammation and immune regulation. *J. Physiol. Pharmacol. 54*, 469−487.

(5) (a) Arnold, E. V., Citro, M. L., Keefer, L. K., and Hrabie, J. A. (2002) A nitric oxide-releasing polydiazeniumdiolate derived from acetonitrile. *Org. Lett. 4*, 1323−1325. (b) Zavorin, S. I., Artz, J. D., Dumitrascu, A., Nicolescu, A., Scutaru, D., Smith, S. V., and Thatcher, G. R. J. (2001) Nitrate esters as nitric oxide donors: ss-Nitrates. *Org. Lett. 3*, 1113−1116. (c) Frost, M. C., and Meyerhoff, M. E. (2004) Controlled photoinitiated release of nitric oxide from polymer films containing S-nitroso-*N*-acetyl-DL-penicillamine derivatized fumed silica filler. *J. Am. Chem. Soc. 126*, 1348−1349.

(6) (a) Tinker, A. C., Beaton, H. G., Boughton-Smith, N., Cook, A. R., Cooper, S. L., Fraser-Rae, L., Hallam, K., Hamley, P., McInally, T., Nicholls, D. J., Pimm, A. D., and Wallace, A. V. (2003) 2-Dihydro-4-quinazolinamines: Potent, highly selective inhibitors of inducible nitric oxide synthase which show anti-inflammatory activity in vivo. *J. Med. Chem. 46*, 913−916. (b) Hallinan, E. A., Hagen, T. J., Bergmanis, A., Moore, W. M., Jerome, G. M., Spangler, D. P., Stevens, A. M., Shieh, H. S., Manning, P. T., and Pitzele, B. S. (2004) 5-Fluorinated L-lysine analogues as selective induced nitric oxide synthase inhibitors. *J. Med. Chem. 47*, 900−906.

(7) Fukuto, J. M., Bartberger, M. D., Dutton, A. S., Paolocci, N., Wink, D. A., and Houk, K. N. (2005) The physiological chemistry and biological activity of nitroxyl (HNO): The neglected, misunderstood, and enigmatic nitrogen oxide. *Chem. Res. Toxicol. 18*, 790−801.

(8) Leaf, C, D., Wishnok, J. S., and Tannenbaum, S. R. (1989) Mechanisms of endogenous nitrosation. *Cancer Surv. 8*, 323−334.

(9) Kim, M. Y., Dong, M., Dedon, P. C., and Wogan, G. N. (2005) Effects of peroxynitrite dose and dose rate on DNA damage and mutation in the *supF* shuttle vector. *Chem. Res. Toxicol. 18*, 76−86.

(10) Zimmermann, F. K. (1977) Genetic effects of nitrous acid. *Mutat. Res. 39*, 127−147.

(11) Suzuki, T., Matsumura, Y., Ide, H., Kanaori, K., Tajima, K., and Makino, K. (1997) Deglycosylation susceptibility and base-pairing stability of 2′-deoxyoxanosine in oligodeoxynucleotide. *Biochemistry 36*, 8013−8019.

(12) Nguyen, T., Brunson, D., Crespi, C. L., Penman, B. W., Wishnok, J. S., and Tannenbaum, S. R. (1992) DNA damage and mutation in human cells exposed to nitric oxide in vitro. *Proc. Natl. Acad. Sci. U.S.A. 89*, 3030−3034.

(13) Pham, P., Bransteitter, R., and Goodman, M. F. (2005) Reward versus risk: DNA cytidine deaminases triggering immunity and disease. *Biochemistry 44*, 2703−2715.

(14) Espey, M. G., Miranda, K. M., Pluta, R. M., and Wink, D. A. (2000) Nitrosative capacity of macrophages is dependent on nitric-oxide synthase induction signals. *J. Biol. Chem. 275*, 11341−11347.

(15) Haorah, J., Zhou, L., Wang, X., Xu, G. P., and Mirvish, S. S. (2001) Determination of total *N*-nitroso compounds and their precursors in frankfurters, fresh meat, dried salted fish, sauces, tobacco and tobacco smoke particulates. *J. Agric. Food Chem. 49*, 6068−6078.

(16) Robichova, S., and Slamenova, D. (2001) Study of *N*-Nitrosomorpholine-induced DNA strand breaks in Caco-2 cells by the classical and modified comet assay: Influence of vitamins E and C. *Nutr. Cancer 39*, 267−272.

(17) Dong, M., Wang, C., Deen, W. M., and Dedon, P. C. (2003) Absence of 2′-deoxyoxanosine and presence of abasic sites in DNA exposed to nitric oxide at controlled physiological concentrations. *Chem. Res. Toxicol. 16*, 1044−1055.

(18) Suzuki, T., Yamaoka, R., Nishi, M., Ide, H., and Makino, K. J. (1996) Isolation and characterization of a novel product, 2′-deoxyoxanosine, from 2′-deoxyguanosine, oligodeoxynucleotide, and calf thymus DNA treated by nitrous acid and nitric oxide. *J. Am. Chem. Soc. 118*, 2515−2516.

(19) Shimada, N., Yagisawa, N., Naganawa, H., Takita, T., Hamada, M., Takeuchi, T., and Umezawa, H. J. (1981) Oxanosine, a novel nucleoside from actinomycetes. *J. Antibiot. 34*, 1216−1218.

(20) Nakamura, H., Yagisawa, N., Shimada, N., Takita, T., Umezawa, H., and Iitaka, Y. J. (1981) The X-ray structure determination of oxanosine. *J. Antibiot. 34*, 1219−1221.

(21) Yagisawa, N., Shimada, N., Takita, T., Ishizuka, M., Takeuchi, T., and Umezawa, H. J. (1982) Mode of action of oxanosine, a novel nucleoside antibiotic. *J. Antibiot. 35*, 755−759.

(22) Uehara, Y., Hasegawa, M., Hori, M., and Umezawa, H. (1985) Increased sensitivity to oxanosine, a novel nucleoside antibiotic, of rat kidney cells upon expression of the integrated viral src gene. *Cancer Res. 45*, 5230−5234.

(23) Itoh, O., Kuroiwa, K., Atsumi, S., Umezawa, K., Takeuchi, T., and Hori, M. (1989) Induction by the guanosine analogue oxanosine of reversion toward the normal phenotype of K-ras-transformed rat kidney cells. *Cancer Res. 49*, 996−1000.

(24) Compare ^{1}H and ^{13}C NMR of the new compound with published data of guanosine in SDBS (http://www.aist.go.jp/RIODB/SDBS/menu-e.html).

(25) Suzuki, T., Yamada, M., Ide, H., Kanaori, K., Tajima, K., Morii, T., and Makino, K. (2000) Identification and characterization of a reaction product of 2-deoxyoxanosine with glycine. *Chem. Res. Toxicol. 13*, 227−230.

(26) (a) Webb, D. R., McDonald, G. G., and Trentham, D. R. (1978) Kinetics of oxygen-18 exchange between inorganic phosphate and water catalyzed by myosin subfragment 1, using the ^{18}O shift in ^{31}P NMR. *J. Biol. Chem. 253*, 2908−2911. (b) Bock, J., and Cohn, M. (1978) Metal dependence of the phosphate (oxygen)-water exchange reaction of *Escherichia coli* alkaline phosphatase. Kinetics followed by ^{31}P(^{18}O) NMR. *J. Biol. Chem. 253*, 4082−4085. (c) Risley, J. M., and Van Etten, R. L. (1978) An ^{18}O isotope shift upon ^{13}C NMR spectra and its application to the study of oxygen exchange kinetics. *J. Am. Chem. Soc. 101*, 252−253.

(27) Jiang, C., Suhadolnik, R. J., and Baker, D. C. (1988) Isotopic shift in an ^{18}O-labeled sugar of adenosine. *Nucleosides Nucleotides 7*, 271−294.

(28) Koch, W., and Holthausen, M. C. (2001) *A Chemist's Guide to Density Functional Theory*, 2nd ed., Wiley-VCH, New York.

(29) Frisch, M. J., Trucks, G. W., Schlegel, H. B., Scuseria, G. E., Robb, M. A., Cheeseman, J. R., Montgomery, J. A., Jr., Vreven, T., Kudin, K. N., Burant, J. C., Millam, J. M., Iyengar, S. S., Tomasi, J., Barone, V., Mennucci, B., Cossi, M., Scalmani, G., Rega, N., Petersson, G. A., Nakatsuji, H., Hada, M., Ehara, M., Toyota, K., Fukuda, R., Hasegawa, J., Ishida, M., Nakajima, T., Honda, Y., Kitao, O., Nakai, H., Klene, M., Li, X., Knox, J. E., Hratchian, H. P., Cross, J. B., Bakken, V., Adamo, C., Jaramillo, J., Gomperts, R., Stratmann, R. E., Yazyev, O., Austin, A. J., Cammi, R., Pomelli, C., Ochterski, J. W., Ayala, P. Y., Morokuma, K., Voth, G. A., Salvador, P., Dannenberg, J. J., Zakrzewski, V. G., Dapprich, S., Daniels, A. D., Strain, M. C., Farkas, O., Malick, D. K., Rabuck, A. D., Raghavachari, K., Foresman, J. B., Ortiz, J. V., Cui, Q., Baboul, A. G., Clifford, S., Cioslowski, J., Stefanov, B. B., Liu, G., Liashenko, A., Piskorz, P., Komaromi, I., Martin, R. L., Fox, D. J., Keith, T., Al-Laham, M. A., Peng, C. Y., Nanayakkara, A., Challacombe, M., Gill, P. M. W., Johnson, B., Chen, W., Wong, M. W., Gonzalez, C., and Pople, J. A. (2003) *Gaussian 03*, Gaussian, Inc., Pittsburgh, PA.

(30) Krishnan, R., Binkley, J. S., Seeger, R., and Pople, J. A. (1980) Self-consistent molecular orbital methods. XX. A basis set for correlated wave functions. *J. Chem. Phys. 72*, 650−654.
(31) Wolinski, K., Hilton, J. F., and Pulay, P. (1990) Efficient implementation of the gauge-independent atomic orbital method for NMR chemical shift calculations. *J. Am. Chem. Soc. 112*, 8251−8260.
(32) Woon, D. E., and Dunning, T. H., Jr. (1993) Gaussian basis sets for use in correlated molecular calculations. III. The atoms aluminum through argon. *J. Chem. Phys. 98*, 1358−1371, and references cited therein.
(33) Cossi, M., Barone, V., Cammi, R., and Tomasi, J. (1996) Ab initio study of solvated molecules: a new implementation of the polarizable continuum model. *Chem. Phys. Lett. 255*, 327−335, and references cited therein.
(34) Velikyan, I., Acharya, S., Trifonova, A., Földesi, A., and Chattopadhyaya, J. (2001) The pK_a's of 2′-hydroxyl group in nucleosides. *J. Am. Chem. Soc. 123*, 2893−2894.
(35) Gaskell, M., Jukes, R., Jones, D. J. L., Martin, E. A., and Farmer, P. B. (2002) Identification and characterization of (3″,4″-dihydroxy)-1,N^2-benzetheno-2′-deoxyguanosine 3′-monophosphate, a novel DNA adduct formed by benzene metabolites. *Chem. Res. Toxicol. 15*, 1088−1095.
(36) (a) Williams, V. R., and Traynham, J. G. (1963) Acid-dissociation of 2-hydroxypyri-dinium ion. *J. Org. Chem. 28*, 2883−2884. (b) Chen, J., and MacKerell, A. D. (2000) Computation of the influence of chemical substitution on the pK_a of pyridine using semiempirical and ab initio methods. *Theor. Chem. Acc. 103*, 483−494.
(37) Chassy, B. M., and Suhadolnik, R. J. (1967) Adenosine aminohydrolase. Binding and hydrolysis of 2- and 6-substituted purine ribonucleosides and 9-substituted adenine nucleosides. *J. Biol. Chem. 242*, 3655−3658.
(38) Wolfenden, R., Kaufman, J., and Macon, J. B. (1969) Ring-modified substrates of adenosine deaminases. *Biochemistry 8*, 2412−2415.
(39) Cristalli, G., Costanzi, S., Lambertucci, C., Lupidi, G., Vittori, S., Volpini, R., and Camaioni, E. (2001) Adenosine deaminase: Functional implications and different classes of inhibitors. *Med. Res. Rev. 21*, 105−128.
(40) Saboury, A. A., Divsalar, A., Ataie, G., Amanlou, M., Moosavi-Movahedi, A. A., and Hakimelahi, G. H. (2003) Inhibition study of adenosine deaminase by caffeine using spectroscopy and isothermal titration calorimetry. *Acta Biochim. Pol. 50*, 849−855.
(41) Rayat, S., Majumdar, P., Peter, T., and Glaser, R. (2004) 5-Cyanoimino-4-oxomethylene-4,5-dihydroimidazole and 5-cyanoamino-4-imidazole-carboxylic acid intermediates in nitrosative guanosine deamination. Evidence from ^{18}O-labeling experiments. *J. Am. Chem. Soc. 126*, 9960−9969.
(42) Rayat, S., and Glaser, R. (2003) 5-Cyanoimino-4-oxomethylene-4,5-dihydroimidazole and nitrosative guanine deamination. A theoretical study of geometries, electronic structures, and N-protonation. *J. Org. Chem. 68*, 9882−9892.
(43) Qian, M., and Glaser, R. (2004) 5-Cyanoamino-4-imidazolecarboxamide and nitrosative guanine deamination: Experimental evidence for pyrimidine ring-opening during deamination. *J. Am. Chem. Soc. 126*, 2274−2275.
(44) Qian, M., and Glaser, R. (2005) Demonstration of an alternative mechanism for G-to-G cross-link formation. *J. Am. Chem. Soc. 127*, 880−887.
(45) (a) Evans, B. E., and Wolfenden, R. V. (1973) Catalysis of the covalent hydration of pteridine by adenosine aminohydrolase. *Biochemistry 12*, 392−398. (b) Sideraki, V., Mohamedali, K. A., Quiocho, F. A., and Rudolph, F. B. (1996) Probing the functional role of two conserved active site aspartates in mouse adenosine deaminase. *Biochemistry 35*, 7862−7872.
(46) (a) Heppel, L. A., Hurwitz, J., and Horecker, B. L. (1956) Adenine deaminase of *Azotobacter vinelandii*. *J. Am. Chem. Soc. 79*, 630−633. (b) Cook, P. F., Hermes, J. D., and Cleland, W. W. (1987) Evidence from nitrogen-15 and solvent deuterium isotope effects on the chemical mechanism of adenosine deaminase. *Biochemistry 26*, 7378−7384. (c) Bhaumik, D., Medin, J., and Coleman, M. S. (1993) Mutational analysis of active site residues of human adenosine deaminase. *J. Biol. Chem. 268*, 5464−5470.
(47) Wolfenden, R. V., and Kirsch, J. F. (1968) Enzymic displacement of oxygen and sulfur from purines. *J. Am. Chem. Soc. 90*, 6849−6850.
(48) Shih, P., and Wolfenden, R. V. (1996) Enzyme−substrate complexes of adenosine and cytidine deaminases: Absence of accumulation of water adducts. *Biochemistry 35*, 4697−4703.
(49) Wilson, D. K., Rudolph, F. B., and Quiocho, F. A. (1991) Atomic structure of adenosine deaminase complexed with a transition-state analog: Understanding catalysis and immunodeficiency mutations. *Science 252*, 1278−1284.
(50) Hudaky, P., and Perczel, A. (2004) Conformation dependence of pK_a: Ab initio and DFT investigation of histidine. *J. Phys. Chem. A 108*, 6195−6205.
(51) Raabe, G., Wang, Y., and Fleischhauer, J. (2000) Calculation of the proton affinities of primary, secondary, and tertiary amines using semiempirical and ab initio methods. *Z. Naturforsch., A: Phys. Sci. 55*, 687−694.
(52) Wang, Z., and Quiocho, F. A. (1998) Complexes of adenosine deaminase with two potent inhibitors: X-ray structures in four independent molecules at pH of maximum activity. *Biochemistry 37*, 8314−8324.
(53) Mima, S. (1963) Proton affinity by electron-impact method, and polymerization reactivity. II. Proton affinities of carbonyl compounds and rearrangement ions from oxygen containing compounds. *Osaka Kogyo Gijutsu Shikensho Kiho 14*, 19−24.
(54) Chang, Z., Nygaard, P., Chinault, A. C., and Kellems, R. E. (1991) Deduced amino acid sequence of *Escherichia coli* adenosine deaminase reveals evolutionarily conserved amino acid residues: implications for catalytic function. *Biochemistry 30*, 2273−2280.
(55) Ford, H., Dai, F., Mu, L., Siddiqui, M. A., Nicklaus, M. C., Anderson, L., Marquez, V. E., and Barchi, J. (2000) Adenosine deaminase prefers a distinct sugar ring conformation for binding and catalysis: Kinetic and structural studies. *Biochemistry 39*, 2581−2592.
(56) Kemp, A. J., Lyons, S. D., and Christopherson, R. I. (1986) Effects of acivicin and dichloroallyl lawsone upon pyrimidine biosynthesis in mouse L1210 leukemia cells. *J. Biol. Chem. 261*, 14891−14895.
(57) Jerome, S., Dussol, B., Fenoulet, E., Capo, C., Mege, J.-L., Halimi, G., Bechis, G., Brunet, P., Rochat, H., Berland, Y., and Guieu, R. (2001) High adenosine and deoxyadenosine concentrations in mononuclear cells of hemodialyzed patients. *J. Am. Soc. Nephrol. 12*, 1721−1728.
(58) Frick, L., and Wolfenden, R. (1986) Transition-state stabilization by adenosine deaminase: Structural studies of its inhibitory complex with deoxycoformycin. *Biochemistry 25*, 1616−1621.
(59) Hong, M. Y., and Hosmane, R. S. (1997) Irreversible, tight-binding inhibition of adenosine deaminase by coformycins: Inhibitor structural features that contribute to the mode of enzyme inhibition. *Nucleosides Nucleotides 16*, 1053−1057.

TX050232H